

# Tough ultrafine-grained Ti through multilayering and grading

D.K. Yang\* and P.D. Hodgson\*

*Institute for Frontier Materials, Deakin University, Waurn Ponds, Victoria 3216, Australia*

Received 1 September 2012; revised 26 October 2012; accepted 30 October 2012

Available online 5 November 2012

The mechanical performance of ultrafine-grained metals can be enhanced through multilayering and grading. The mechanical gradation across the layers and in the junctions between layers achieves a more gradual stress redistribution, providing robustness to catastrophic failure. A mechanics model is established to explain the crack-stopping effect of the multilayers. The material design principal reported here provides a valuable guide for the development of the nanogained/ultrafine-grained materials with high strength and toughness.

© 2012 Acta Materialia Inc. Published by Elsevier Ltd. All rights reserved.

**Keywords:** Ultrafine-grained materials; Toughening; Multilayering; Grading

Reducing the grain size of a materials to the ultrafine-grained (UFG) or nanogained (NG) scale can enhance their mechanical strength by up to an order of magnitude [1]. These tremendous gains in strength are the result of the large population of grain boundaries, which delay yielding by obstructing the formation and movement of dislocation inside the crystalline lattices [2]. Although UFG or NG materials exhibit excellent mechanical strength and high hardness, most have limited plasticity [2,3]. This drawback leads to their limited applicability and high susceptibility to catastrophic failure in load-bearing applications. Several recent successful strategies to toughen UFG metals without significantly sacrificing strength include producing a non-uniform/composite microstructure formed in situ [4–7], testing at high strain rates and/or lower temperatures [8], and producing an NG structure with a large fraction of high-angle grain boundaries and a low dislocation density [9].

Surface deformation by rolling or shot-peening induces residual stress at the surface layer. For conventional engineering alloys, in which brittle fracture is not the failure mode, the effect of surface residual stress is not strengthening, but instead an increase in fatigue resistance [10]. For brittle materials, such as ceramic and inorganic glass, where failure is through brittle fracture, and the surface residual stress improves the strength [11]. The sensitivity to defects and lack of ductility of UFG materials provide some similarities with conventional ceramic

or glass. The macroscopic plastic deformation of UFG material has been known to be accomplished by the formation and evolution of shear bands, in which a high amount of plastic flow is localized within a rather narrow region [1,3]. With extensive exploitation of the laminated structure and residual stress in ceramic or glass [10,11], as well as several good examples of graded structures achieved in conventional coarse-grained metals [12–16], it is strange that the effects of multilayering and surface residual stress in UFG or NG metals have been little explored. In addition, fabrication of UFG Ti by means of severe plastic deformation has been successfully achieved by many researchers during the past decade [17–20]. The aim of this study is to apply cryorolling and the surface mechanical attrition treatment (SMAT) [12] to commercial-purity Ti to engineer a multilayered hierarchical structure (MHS) and to evaluate the effects of this structure, in particular the multilayering and grading, with regard to its mechanical behavior.

A grade 2 Ti plate with a mean grain size of around 60  $\mu\text{m}$  was cryogenically rolled from 36 to 5 mm thickness with a reduction of  $\sim 2$  mm per pass. The workpiece was then cut parallel to the rolling direction (RD) and polished to a rectangular bar with dimensions of  $5 \times 5 \times 90 \text{ mm}^3$ . Subsequently, the four lateral surfaces of the rectangular bar were subjected to SMAT in sequence. The SMAT process was performed in a low vacuum using hardened stainless steel balls (8 mm in diameter) at a vibration frequency of 50 Hz for 60 min for each side. Rectangular specimens with dimensions of  $5 \times 5 \times 10 \text{ mm}^3$  were tested under uniaxial compression along the RD at a strain rate of

\* Corresponding authors. Tel.: +61 3 5227 1283 (D.K. Yang), +61 3 5227 1251 (P.D. Hodgson); e-mail addresses: [dengke.yang@research.deakin.edu.au](mailto:dengke.yang@research.deakin.edu.au); [peter.hodgson@deakin.edu.au](mailto:peter.hodgson@deakin.edu.au)

$5 \times 10^{-4} \text{ s}^{-1}$  in an Instron 100 kN machine at room temperature. Nanoindentation experiments were conducted at ambient temperature using an UMIS indentation system at a strain rate of  $5 \times 10^{-2} \text{ s}^{-1}$  and a maximum load of 20 mN. Microstructural observations were conducted using a Zeiss Supra 55VP field-emission gun scanning electron microscope operated at 10 kV and a Jeol JEM 2100 transmission electron microscope operated at 200 kV. A Panalytical X'Pert XRD instrument with Cu  $K_\alpha$  operated at 45 kV/35 mA was employed to measure the residual stress–depth profile by using the  $\sin^2 \phi$  method in combination with sublayer removal. The lattice strains were calculated from the [213] diffraction peak at a diffraction angle of around  $139.5^\circ$ . The detailed principles and experimental procedures for determination of residual stress using XRD can be found in Refs. [21,22].

The material (Ti, grade 2) reported here has an MHS consisting of three different parts: an outer amorphous/nanocrystallite (A/NC) layer (thickness  $\sim 30 \mu\text{m}$ ), a middle nanograined (NG) layer (thickness  $\sim 60 \mu\text{m}$ ) and an innermost UFG core (Fig. 1a). Transmission electron microscopy (TEM) analysis revealed that the top layer was composed of a bright amorphous matrix and a discrete darker nanostructure (Fig. 1b). The middle layer consisted of nanograins with an average size of  $\sim 40 \text{ nm}$  (Fig. 1c). The UFG core, as shown in Fig. 1d, is composed of ultrafine equiaxed grains with a grain size distribution in the range of 50–250 nm. The hardness and modulus, obtained by nanoindentation, decrease from the outer to the inner layers (Fig. 2a), in correspondence with the microstructural characteristics of MHS.

Figure 2b shows the engineering stress–strain curves of MHS Ti compared with UFG Ti. The toughness can be established by measuring the area underneath the stress–strain curve [23]. The enhanced strength and the area under the stress–strain curve shown in Figure 2b demonstrate an obvious concurrent strengthening and toughening of UFG Ti by modifying the MHS. The yield strength is approximately the same for the UFG Ti and the MHS Ti, but in the latter there is a significant increase in strength, concurrent with a slight improvement in ductility.

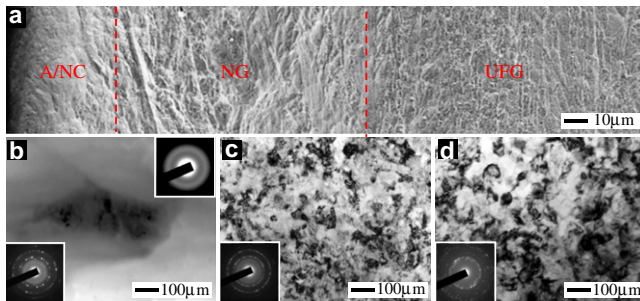


**Figure 1.** (a) SEM image of the specimen cross-section, showing that MHS Ti consists of three different layers: A/NC, NG and UFG core. (b) TEM bright-field (BF) image of the microstructures 20  $\mu\text{m}$  below the top surface. The upper right inset is the selected-area diffraction (SAD) pattern of the amorphous phase and the lower left inset is the SAD pattern of the nanocrystallite; (c) TEM BF image of the microstructure 60  $\mu\text{m}$  below the top surface; the inset shows the corresponding SAD pattern; (d) TEM BF image of the UFG core; the inset shows the corresponding SAD pattern.

To obtain an insight into the toughening mechanism, one lateral surface of the specimen was polished to a mirror finish to remove the A/NC and NG layers and the specimen was subsequently subjected to different compression strains. Obvious localized shear regions can be observed in the UFG core, whereas the NG layer displays a uniform morphology without any localized shear after 5% deformed strain (Fig. 3a). This observation provides evidence that the localized shear initiated in the UFG core instead of the NG layer. Figure 3b reveals that localized shear, which originated in the UFG core, piled up and was hindered at the junction of the NG layer and UFG core (NG/UFG) during deformation. Figure 3c shows a crack that propagated across the entire UFG core but was arrested and bifurcated at the NG/UFG interface after 30% deformation. These experimental observations suggest that the NG structure might have significant intrinsic deformation ability and that the cracks nucleate in the UFG core and propagate preferentially toward the NG layer during the compression deformation, as supported by the work of Fang et al. [24].

The complex residual stresses can be introduced into the materials through sequentially combining cryorolling and SMAT [13,25,26]. The residual stress–depth profile (Fig. 2c) shows that moderate compressive stresses occur in the surface adjacent layer, followed by large tensile stresses over the junction of NG/UFG. Beyond the junction of NG/UFG, the stresses increase and eventually become compressive. Figure 3 shows that cracks were arrested and bifurcated at the NG/UFG interface. These observations suggest the development of a toughening model to explain the crack-stopping effect of the UFG/NG interface.

Suppose that the MHS Ti, composed of  $t_1$  thick reinforcing layers, is subjected to residual tensile stress  $\sigma_t$  and that the  $t_2$  thick UFG core is subjected to residual compressive stress  $\sigma_c$ , all of which are subjected to an applied compressive stress  $\sigma_a$ . The analysis is based on the calculation of the stress intensity factor  $K$  for a propagating crack of length  $2a$  spanning the sandwich, inclined at an angle of  $\beta$  relative to the horizontal line (Fig. 4a), when it extends into the NG/UFG interface region  $t_2 \leq 2a \leq t_2 + 2t_1$ . The stress parallel to the specimen can be resolved into two components, as schematically illustrated in Figure 4d. These stress components are:  $\sigma_y = \sigma \cos^2 \beta$  and  $\tau_x = \frac{\sigma}{2} \sin 2\beta$ .

The stress intensity factor  $K_a$  for the crack in Figure 4a is determined by superimposing the two stress fields shown in Figure 4b and c. Using the rule of superimposition [27,28], the stress intensity factor  $K_a$  is the sum of the stresses generated by the decomposed stress fields of  $K_b$  and  $K_c$ .

$$K_a = K_b + K_c \quad (1)$$

$K_b$  is the stress intensity factor for a compressive stress field with a magnitude of  $\sigma_a - \sigma_t$  applied to the whole specimen that does not contain residual stresses (Fig. 4b).  $K_c$  is the stress intensity factor for a compressive stress field of magnitude  $\sigma_c - \sigma_t$  applied cross the UFG core (Fig. 4c).

The stress intensity factor for  $K_b$  is determined as [28]

$$K_{Ib} = (\sigma_a - \sigma_t) \cos^2 \beta \sqrt{\pi a} \quad (2)$$

Download English Version:

<https://daneshyari.com/en/article/1498819>

Download Persian Version:

<https://daneshyari.com/article/1498819>

[Daneshyari.com](https://daneshyari.com)